The Journal of Neuroscience, October 15, 1999, *19*(20):8830–8838

Domains Responsible for Constitutive and Ca^{2+}-Dependent Interactions between Calmodulin and Small Conductance Ca^{2+}-Activated Potassium Channels

John E. Keen,[1] Radwan Khawaled,[1] David L. Farrens,[2] Torben Neelands,[1] Andre Rivard,[1] Chris T. Bond,[1] Aaron Janowsky,[4] Bernd Fakler,[5] John P. Adelman,[1] and James Maylie[3]

[1]Vollum Institute, [2]Departments of Biochemistry and Molecular Biology, [3]Obstetrics and Gynecology, and [4]Research Service, Veteran's Administration Medical Center, and Department of Psychiatry, Behavioral Neuroscience, and Physiology and Pharmacology, Oregon Health Sciences University, Portland Oregon, 97201, and [5]Department of Physiology, University of Tüebingen, Tüebingen, Germany

Small conductance Ca^{2+}-activated potassium channels (SK channels) are coassembled complexes of pore-forming SK α subunits and calmodulin. We proposed a model for channel activation in which Ca^{2+} binding to calmodulin induces conformational rearrangements in calmodulin and the α subunits that result in channel gating. We now report fluorescence measurements that indicate conformational changes in the α subunit after calmodulin binding and Ca^{2+} binding to the α subunit–calmodulin complex. Two-hybrid experiments showed that the Ca^{2+}-independent interaction of calmodulin with the α subunits requires only the C-terminal domain of calmodulin and is mediated by two noncontiguous subregions; the ability of the E-F hands to bind Ca^{2+} is not required. Although SK α subunits lack a consensus calmodulin-binding motif, mutagenesis experiments identified two positively charged residues required for Ca^{2+}-independent interactions with calmodulin. Electrophysiological recordings of SK2 channels in membrane patches from oocytes coexpressing mutant calmodulins revealed that channel gating is mediated by Ca^{2+} binding to the first and second E-F hand motifs in the N-terminal domain of calmodulin. Taken together, the results support a calmodulin- and Ca^{2+}-calmodulin-dependent conformational change in the channel α subunits, in which different domains of calmodulin are responsible for Ca^{2+}-dependent and Ca^{2+}-independent interactions. In addition, calmodulin is associated with each α subunit and must bind at least one Ca^{2+} ion for channel gating. Based on these results, a state model for Ca^{2+} gating was developed that simulates alterations in SK channel Ca^{2+} sensitivity and cooperativity associated with mutations in CaM.

Key words: SK channels; afterhyperpolarization; calmodulin; Ca^{2+}-gating; Ca^{2+}-independent interactions; state model

SK channels are potassium-selective, voltage-independent, and are activated by increases in the levels of intracellular Ca^{2+} such as occur during an action potential. SK channels underlie the slow afterhyperpolarization (sAHP; Blatz and Magleby, 1987; Sah, 1996) that limits the firing frequency during a train of action potentials (Madison and Nicoll, 1984; Lancaster and Adams, 1986; Hille, 1992; Sah, 1996). This spike-frequency adaptation regulates burst frequency and is essential for normal integrative neurotransmission.

Three mammalian SK channels (SK1, SK2, and SK3) have been cloned that demonstrate a high degree of structural homology (Köhler et al., 1996) and a high sensitivity to Ca^{2+}. The channels gate rapidly after application of saturating Ca^{2+}, with onset of current commencing within 1 msec, a time course of activation similar to that observed for other ligand-gated channels such as GABA (Maconochie et al., 1994) or ionotropic glutamate receptors (Lester et al., 1990), suggesting a direct interaction between the ligand (Ca^{2+} ions) and the channel protein. Structure–function analysis revealed that Ca^{2+}-gating is accomplished by constitutive association of calmodulin (CaM) with a region of the channel α subunits, ABC (SK2, amino acids 390–487), which resides in the intracellular C-terminal domain, and a Ca^{2+}-dependent interaction with the BC region (SK2, amino acids 423–487). A model was presented in which Ca^{2+} ions bind to CaM, inducing conformational changes that are transmitted to the channel α subunits, resulting in channel activation (Xia et al., 1998).

CaM is a ubiquitous mediator of Ca^{2+}-dependent processes. CaM contains N- and C-terminal globular domains, each including two high-affinity Ca^{2+}-binding E-F hand motifs, E-F 1 and 2 in the N terminus, and E-F 3 and 4 in the C terminus (Babu et al., 1985). Ca^{2+} ions bind to CaM in a highly cooperative manner, first to E-F 4 and 3 and subsequently to E-F 2 and 1. Ca^{2+} binding to CaM induces conformational rearrangements that bend the linker region and bring the globular domains into close proximity. In addition, hydrophobic side chains within each globular domain are exposed. Taken together, these structural alterations present a physical interface for a diverse spectrum of signaling substrates important in developmental and adaptive responses among virtually all cell types, as well as synaptic plasticity in the mammalian CNS (O'Neil and DeGrado, 1990).

The interaction between CaM and SK channel α subunits is

Received June 11, 1999; revised Aug. 5, 1999; accepted Aug. 10, 1999.

This work was supported by grants from the National Institutes of Health, the Muscular Dystrophy Association, Human Frontier Science Program, and ICAgen, Inc. We thank Mr. Robert Johnson for assistance with ^{125}I-apamin binding experiments. We also thank Drs. Xia-Ming Xia and Takahiro Ishii for some of the mutagenesis and fruitful discussions.

Drs. Keen and Khawaled contributed equally to this work.

Correspondence should be addressed to Dr. James Maylie, Department of Obstetrics and Gynecology, Oregon Health Sciences University, 3181 Southwest Sam Jackson Park Road, Portland, OR 97201.

constitutive and is maintained in the presence or the absence of Ca^{2+} ions (Xia et al., 1998). This permits a direct coupling between changes in intracellular Ca^{2+} concentrations and changes in membrane potential. The results of experiments reported here revealed a modular strategy in which the N-terminal E-F hands of CaM are responsible for Ca^{2+}-induced conformational changes in the channel, whereas two short stretches of amino acids in the C-terminal half of CaM mediate constitutive interactions.

MATERIALS AND METHODS

Molecular biology. Site-directed mutagenesis was performed as described (Weiner et al., 1994) using pfu DNA polymerase (Stratagene, La Jolla, CA); mutations were verified by DNA sequence analysis. The Genetics Computer Group suite of programs was used for DNA and protein sequence analysis. For oocyte expression, all mRNAs were derived from sequences that were subcloned into the oocyte expression vector pBF. To join subunits in tandem, the relevant stop codon was removed, and a linker encoding 10 glutamine residues (Q_{10}) was inserted between the last codon of the 5′ subunit coding sequence and the initiator codon of the following subunit. This was achieved using a sequential PCR protocol modified from Horton et al. (1989); junctions were generated by overlap extension of PCR primers that also encoded the glutamine linkers (Pessia et al., 1996).

Fusion proteins and Western blots. The indicated channel sequences (SK2 or SK2R464E,K467E, ABC or BC) were amplified by PCR using pfu DNA polymerase (Stratagene) and subcloned into the glutathione *S*-transferase (GST) fusion vector pGEX-KG (Pharmacia Biotech, Piscataway, NJ). Cultures harboring the plasmids were harvested in PBS and lysed by French press. Cleared lysates were incubated with glutathione agarose (Sigma, St. Louis, MO) for 2 hr at 4°C, and the resin was subsequently washed twice with PBS in the presence (10 μM) or absence (5 mM EGTA) of Ca^{2+}. Resin-bound proteins were incubated with purified bovine brain CaM (generous gift of Dr. Debra Brickey, Vollum Institute) in the presence or absence of Ca^{2+} for 2 hr at 4°C. The resin was then washed twice with PBS with or without Ca^{2+}. Bound proteins were eluted using 10 mM reduced glutathione (Sigma) in 50 mM Tris, pH 8.0. SDS-PAGE (14% acrylamide) was performed with 0.5 mM EGTA in the gel and running buffer. For Western blotting, proteins were electroblotted to Hybond membrane (Amersham, Arlington Heights, IL), and CaM was detected using a monoclonal antibody (Upstate Biotechnology, Lake Placid, NY) and HRP-linked secondary antibody (Bio-Rad, Hercules, CA), visualized with chemiluminescence (New England Nuclear, Boston, MA).

For fluorescence emission measurements, SK2 ABC (Xia et al., 1998) was subcloned into pET33b and produced in *Escherichia coli* BL21 as a his(6)-fusion protein. Ni^{2+}-agarose purification resulted in a single coomassie-stained band after SDS gel electrophoresis. Purified ABC was dialyzed into 360 mM NaCl, 1 mM EGTA, and 18 mM HEPES, pH 7.2.

Fluorescence emission measurements. Fluorescence emission spectra were performed using a Photon Technologies QM-1 steady-state fluorescence spectrophotometer. Samples were excited at 295 nm (2 nm bandpass), and the fluorescence emission was monitored in 1 nm intervals from 310 to 410 nm (5 nm bandpass). Measurements were performed at 22°C, in 360 mM NaCl, 1 mM EGTA, and 18 mM HEPES, pH 7.2. A typical measurement used 1.4 μM of ABC peptide in the above buffer. CaM was added from a stock of 120 μM to an ~1:1.25 ratio with the ABC peptide. To this solution $CaCl_2$ was added from a 1 M stock (Fluka, Milwaukee, WI) to a final concentration of 1.1 mM, yielding a final free Ca^{2+} concentration of 100 μM.

Yeast two-hybrid. The indicated SK2 α subunit coding sequences were subcloned into the bait vector pPC97 as fusions with the GAL4 DNA binding domain. Rat CaM, subfragments, or point mutations (as indicated in the text), were fused to the transcriptional activator domain in the prey vector pPC86 (Chevray and Nathans, 1992). HF7c competent yeast were cotransformed with each of the indicated plasmids, and transformants were plated onto media lacking leucine and tryptophan. From this plate, a single colony was grown overnight in leu^-, trp^- liquid media. The next morning, the culture was diluted 100-fold with 10 mM Tris, 0.1 mM EDTA, and interactions between the bait and prey were assessed by spotting 1 μl onto leu^-, trp^-, his^- plates. Growth was monitored after 2 d of incubation at 30°C.

^{125}I-apamin binding. Oocytes were rinsed in ice-cold assay buffer (100 mM Tris-HCl, 1 mM EDTA, 5.4 mM KCl, and 1% BSA, pH. 8.4, at 4°C), and then added to wells containing ^{125}I-apamin (0.1–1.4 nM) (New England Nuclear) and assay buffer in a final volume of 750 μl. After 1 hr of incubation, oocytes were rinsed in four changes of ice-cold assay buffer over a total of 15 sec, placed on filter paper, and binding was detected on a PhosphorImager.

In the same experiment, radioligand binding was quantified for individual oocytes by conventional gamma ray spectrometry. Specific binding was defined as the difference in radioligand binding observed in the absence and presence of 10 nM apamin (Sigma). Under these conditions, bound radioligand accounted for <10% of total radioligand added to the assay.

Electrophysiology. In vitro mRNA synthesis and oocyte injections were performed as previously described (Xia et al., 1998). *Xenopus* care and handling were in accordance with the highest standards of institutional guidelines. Patch recordings in the inside-out configuration were made at room temperature (~23°C) 3–7 d after injection. Pipettes prepared from thin-walled borosilicate glass (World Precision Instruments, Sarasota, FL) had resistances of 0.5–2 MΩ when filled with (in mM) 120 K-methanesulfonate (MES) and 5 HEPES, pH-adjusted to 7.2 with KOH. Voltage-clamp recordings were performed with an Axopatch 1B or Axopatch 200A patch-clamp amplifier (Axon Instruments, Foster City, CA). Currents were sampled at 2 kHz and filtered at 2 kHz (−3 dB). Excised patches were superfused with an intracellular solution containing (in mM): 120 K-MES, 5 HEPES, and 1 EGTA, which was supplemented with $CaCl_2$, pH-adjusted to 7.2 with KOH; the amount of $CaCl_2$ required to yield the concentrations indicated was calculated according to Fabiato and Fabiato (1979). Solutions were prepared with HEPES (Life Technologies, Gaithersburg, MD), 1 M KOH standard solution (Fluka, Milwaukee, WI), methanesulfonic acid (Aldrich, Milwaukee, WI), EGTA (Fluka), and 1 M $CaCl_2$ (BioChemika MicroSelect; Fluka). Currents within a concentration response obtained early after patch excision were subject to rundown (<20%), which would bias the EC_{50} (Ishii et al., 1997). Therefore, current amplitudes were corrected for rundown by normalizing to the control current predicted from the time course of rundown of the current activated by 10 μM Ca^{2+}. Ca^{2+} dose–response curves were determined from current amplitudes measured at −80 mV as a function of Ca^{2+} concentration and fit with a Hill equation. The values are reported as the mean EC_{50} ± SD of n experiments, as indicated. Statistical significance was evaluated using a paired t test, and a p value <0.01 was considered significant. Data analysis was performed using Pulse (Heka, Lambrecht, Germany) and Igor (Wavemetrics, Lake Oswego, OR). Simulation of Ca^{2+}-dependent activation of SK2 was modeled using SCoP (Simulation Resources, Berrien Springs, MI) running in a DOS environment on a Power Macintosh (Virtual PC; Connectix, San Mateo, CA).

RESULTS

CaM-mediated structural rearrangments in the SK2 ABC

The ABC domain of SK2 was purified from bacteria and used for fluorescence emission measurements (Lakowicz, 1983). This region of the channel α-subunit contains a single tryptophan residue, W432, which resides in a highly solvent-exposed environment, as judged by its fluorescence emission maximum at 346.2 ± 0.8 nm (n = 5; Fig. 1). CaM could be added to this peptide in the absence of Ca^{2+} to induce a complex that saturated (data not shown), indicating a specific interaction between ABC and CaM. The CaM binding to ABC shifted the fluorescence emission to 329.0 ± 0.0 nm (n = 5) and increased its fluorescence intensity by a factor of 4.1 ± 0.1 (n = 5; Fig. 1*B*). These results indicate that CaM binding introduces W432 into a more hydrophobic environment. After addition of Ca^{2+}, yielding a free Ca^{2+} concentration of 100 μM, to the ABC–CaM complex, a large decrease in fluorescence was observed that returned the total intensity to 1.5 ± 0.1 that of the original level (Fig. 1*C*). Interestingly, this decrease was accompanied by a further shift in the emission maxima to 326.2 ± 0.4 nm (n = 5). This latter result indicates that W432 remained in a hydrophobic environment and suggests a static quenching mechanism. Importantly, the fluorescence shift

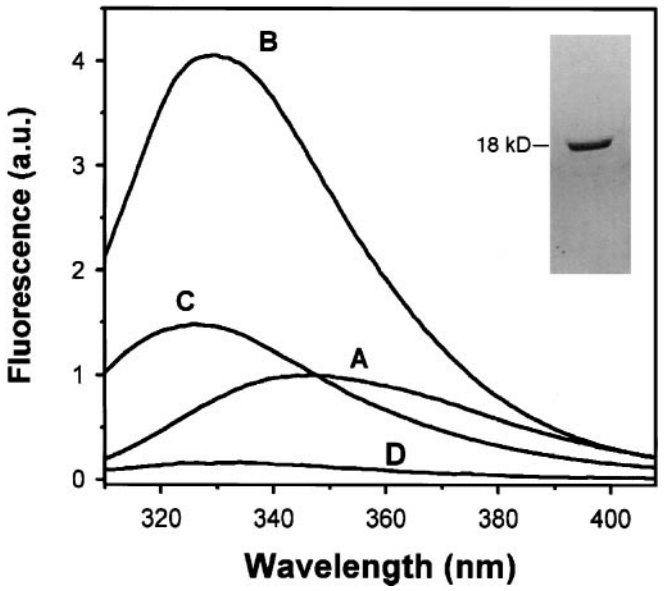

Figure 1. Fluorescence properties of the ABC peptide in presence of CaM and $CaCl_2$. *A,* Fluorescence spectrum of 1.4 μM ABC peptide in the absence of Ca^{2+}. *B,* Spectrum of 1.4 μM ABC peptide combined with 2.1 μM CaM in the absence of Ca^{2+}. Notice the increase and blue shift of fluorescence. *C,* Addition of 1.1 mM $CaCl_2$ to the sample in *B*, resulting in a free Ca^{2+} concentration of 100 μM. All spectra were taken at 22°C using 295 nm excitation, in a buffer solution of (in mM): 360 NaCl, 18 HEPES, and 1 EGTA, pH 7.2. The spectra represent an average of five measurements. For each measurement, the buffer spectrum was subtracted. *D,* The spectrum of 2.1 μM CaM in the absence of the ABC peptide. No shift in fluorescence was observed after addition of Ca^{2+} to the ABC peptide alone (data not shown), indicating that the shift observed in *C* is caused by binding of Ca^{2+} to the ABC–CaM complex. The *inset* shows a silver-stained polyacrylamide gel of the purified ABC peptide used in this study.

observed after addition of Ca^{2+} shows that CaM remains bound to the ABC peptide in the presence of Ca^{2+}, because no wavelength shift was observed after addition of Ca^{2+} to the ABC peptide alone (data not shown). Taken together, these results demonstrate that (1) CaM binding to ABC induces a change in the environment of W432, and (2) subsequent Ca^{2+} binding to the ABC–CaM complex further alters the conformation of ABC.

CaM domains required for Ca^{2+}-independent interactions with SK2 ABC

Two-hybrid experiments detected an interaction between CaM and the ABC domain of the SK2 channel α subunits, but not between CaM and the BC domain. In contrast, an interaction between CaM and the BC domain was detected biochemically using the purified proteins, but only in the presence of Ca^{2+} (Xia et al., 1998; our unpublished results) indicating that the two-hybrid system detects only the Ca^{2+}-independent interactions between CaM and the SK2 α subunits. To determine regions of CaM responsible for Ca^{2+}-independent interactions with SK2 α subunits, fragments of CaM were tested for their ability to complement different domains of the SK2 intracellular C-terminal domain in two-hybrid experiments. Consistent with previous results, only α subunit fragments containing ABC showed complementation with any of the CaM fragments tested. When CaM was divided approximately in half, the N-terminal fragment (amino acids 1–82) was ineffective for complementation with ABC from SK2, whereas the C-terminal fragment (amino acids 78–148) complemented ABC (Fig. 2*A*). To further define residues important for the interaction, truncations from amino acid D78 or from the C terminus, amino acid K148, were tested. Removal of seven residues (amino acids 78–85) from the N terminus or five residues (amino acids 143–148) from the C terminus eliminated the ability of the CaM fragment to complement ABC from SK2 (Fig. 2*A*). Moreover, intact CaM with D→A mutations in any or all combinations of the E-F hands complemented ABC from SK2 (Fig. 2*B*), indicating that functional Ca^{2+}-binding motifs are not required for the constitutive interaction of CaM with SK2ABC.

A.

CaM Fragments	SK2 ABC
1-148	+
1-132	–
1-113	–
1-96	–
1-82	–
1-59	–
1-46	–
1-24	–
27-148	+
27-132	–
27-96	–
27-59	–
42-148	+
42-113	–
42-82	–
63-148	+
63-132	–
63-96	–
78-148	+
78-113	–
78-143	–
85-148	–
100-148	–
100-132	–
109-148	–
136-148	–

B.

CaM	SK2 ABC
W.T.	+
E-F 1	+
E-F 2	+
E-F 3	+
E-F 4	+
E-F 1,2	+
E-F 3,4	+
E-F 1,2,3	+
E-F 1,2,4	+
E-F 1,3,4	+
E-F 2,3,4	+

Figure 2. CaM domains involved in constitutive binding to SK2 α subunits. *A,* Fragments of CaM tested for interaction with SK2 ABC domains in the yeast two-hybrid assay. The C-terminal 70 amino acids of CaM showed complementation, but removal of residues 78–84 or 144–148 from this fragment resulted in the loss of the interaction. *B,* E-F hands are not required for the constitutive interaction between CaM and SK2 ABC in the two-hybrid assay. Wild-type CaM or CaM with the D→A mutation in the indicated E-F hands were tested for interaction with the ABC domain of SK2 in the two-hybrid assay. The interaction was detected in all cases.

SK2 residues necessary for Ca^{2+}-independent interactions with CaM

To identify sites on the SK2 α subunit that interact with CaM, a series of point mutations in the SK2 ABC domain was generated. All charged residues were altered by site-directed mutagenesis but yielded functional channels with Ca^{2+} responses similar to wild type (Xia et al., 1998; data not shown). Several double mutations were constructed and one double mutant, R464E,K467E in the C helix, did not yield functional channels. These positions are conserved as positively charged amino acids in all SK

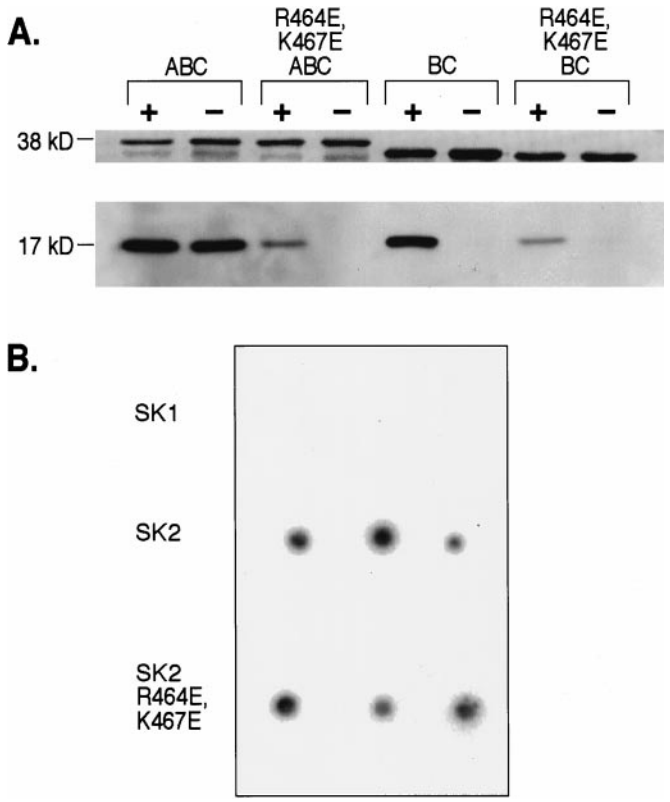

Figure 3. SK2R464E, K467E does not constitutively bind CaM but forms apamin receptors in the plasma membrane. *A,* GST pulldown experiments. GST fusion proteins of ABC or BC domains from SK2 or SK2R464E, K467E were tested for their ability to interact with CaM in the presence (+; 10 μM Ca^2) or absence (−; 5 mM EGTA) of Ca^{2+}. Duplicate gels were prepared with equal amounts of eluted proteins. One gel was silver-stained showing intact GST-fusion proteins (*top*), and the other was used for Western blotting (*bottom*) with an antibody to CaM. SK2 ABC bound CaM under either condition, whereas BC bound CaM only in the presence of Ca^{2+}. CaM bound to SK2R464E, K467E ABC weakly in the presence but not in the absence of Ca^{2+}. *B,* Phosphorimage of ^{125}I-apamin binding to single intact oocytes. No specific ^{125}I-apamin binding was detected for oocytes expressing SK1 channels, whereas oocytes expressing apamin-sensitive SK2 channels and oocytes injected with mRNA encoding SK2R464E, K467E showed specific ^{125}I-apamin binding.

α-subunits. To examine the basis for the lack of function, GST fusion proteins of the wild-type ABC or ABC(R464E,K467E) were tested for their ability to interact with CaM in the presence (10 μM) or absence (5 mM EGTA) of Ca^{2+}. The results showed that wild-type ABC bound CaM under either condition, whereas wild-type BC bound CaM only in the presence of Ca^{2+} (Xia et al., 1998). In contrast, ABC(R464E,K467E) or BC(R464E,K467E) bound CaM only in the presence of 10 μM Ca^{2+} (Fig. 3*A*). Less binding of CaM to the double mutant proteins compared to wild type was observed, suggesting that even the Ca^{2+}-dependent interaction was weakened by these mutations. Consistent with these results, an interaction of the ABC(R464E,K467E) double mutant with CaM was not detected in a two-hybrid test (data not shown). To determine whether R464E,K467E channels were assembled and inserted in the plasma membrane, or whether the double mutation affected channel biosynthesis, ^{125}I-apamin binding studies were performed on intact oocytes injected with mRNA encoding apamin-insensitive SK1 channels, apamin-sensitive SK2 channels, or SK2 R464E,K467E channels. SK1 channels showed no specific binding, but ^{125}I-apamin binding was clearly seen for oocytes expressing either SK2 (specific binding, 2406 cpm; $n = 3$) or SK2 R464E,K467E (specific binding, 2645 cpm; $n = 3$; Fig. 3*B*). These results indicate that R464 and K467 in SK2 are necessary for the constitutive interaction between SK2 and CaM.

To examine the stoichiometry of CaM required for channel function, SK1 (Köhler et al., 1996; Xia et al., 1998) and SK2(R464E,K467E) subunits were linked together by a 10 glutamine linker (Q_{10} linker), and the dimer mRNA was injected into *Xenopus* oocytes. In contrast to expression of a dimer of SK1 and wild-type SK2 (Ishii et al., 1997), channel gating was not observed from oocytes injected with SK1-SK2(R464E,K467E) dimer mRNA, even though ^{125}I-apamin binding sites were detected on the surface membrane (data not shown). This result suggests that CaM must be bound constitutively to at least three α subunits for channel function.

Ca^{2+}-dependent channel gating is mediated by E-F hands 1 and 2

The aspartate residue found in the first position of each E-F hand of rat CaM was altered by site-directed mutagenesis to an alanine (D→A), either alone or in all possible combinations. Previous results established that this mutation dramatically reduced or abolished Ca^{2+} binding (Geiser et al., 1991; Xia et al., 1998). Wild-type or mutant CaMs were coexpressed with SK2 in *Xenopus* oocytes, and Ca^{2+}-gating was examined in inside-out macropatches. Application of Ca^{2+} to patches from oocytes coexpressing wild-type CaM and SK2 resulted in Ca^{2+}-activated potassium currents with an EC_{50} of 0.38 ± 0.05 μM and a Hill coefficient of 4.6 ± 1.3 ($n = 23$). Neither the EC_{50} nor current amplitudes were different from oocytes expressing SK2 alone or coexpressing SK2 and wild-type CaM (Xia et al., 1998). Mutations of D→A in either E-F hand 1 or 2 (CaM1 or CaM2) shifted the EC_{50} to higher Ca^{2+} concentrations and reduced the Hill coefficient, whereas mutations in either E-F hands 3 or 4 (CaM3 or CaM4) did not significantly alter Ca^{2+}-dependent gating of SK2 (Fig. 4, Table 1). Coexpression of SK2 with CaM harboring D→A mutations in both E-F hands 1 and 2 (CaM12) resulted in small currents that on average were 0.05 ± 0.03 ($n = 12$) of current amplitudes observed in coexpression of SK2 with wild-type CaM. The Ca^{2+} concentration–response curve was slightly shifted, but because of the small size of the current compared to background, this difference may not be significant. Similar results were obtained from coexpression of SK2 with CaM harboring mutations in all four E-F hands, indicating that the current in oocytes injected with SK2 and CaM12 or CaM1234 may result from SK2 channels coassembled with endogenous oocyte CaM. In contrast, coexpression of SK2 with CaM34 resulted in robust currents with Ca^{2+} concentration–response relationships not different from SK2 coexpressed with wild-type CaM (Fig. 4, Table 1). These results show that the double mutation in both E-F hands 1 and 2 suppress channel function, whereas mutations in either E-F hands 1 or 2 shifted the EC_{50} and reduced the Hill coefficient for Ca^{2+} activation. To test whether only a single functional E-F hand was sufficient for channel activation, SK2 was coexpressed with mutant CaMs with three of the four E-F hands bearing the D→A mutation. Coexpression of SK2 with CaM123 or CaM124 resulted in currents similar to those resulting from coexpression of SK2 with CaM12 or CaM1234. However, coexpression of SK2 with CaM134 or CaM234 resulted in robust currents with right-shifted EC_{50} values and reduced Hill coefficients similar to mutations in E-F hands 1 or 2 (Table 1). These results show that

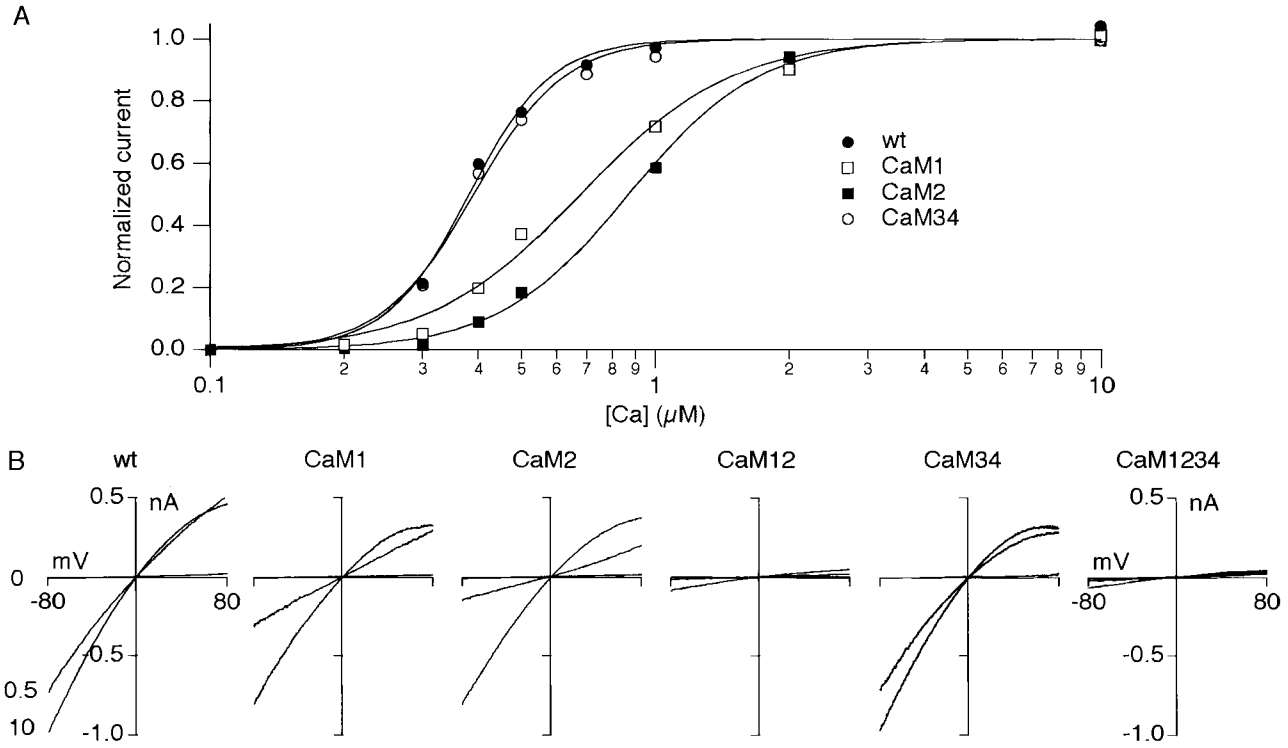

Figure 4. Domains of calmodulin responsible for SK2 gating. *A,* Representative Ca^{2+}-response curves of SK2 coexpressed with the indicated CaM molecules. Relative current amplitudes measured at −80 mV were plotted versus the intracellular Ca^{2+} concentration for the indicated CaM molecules. The data were fitted with a Hill equation (*continuous lines*) yielding an EC_{50} of 0.38 μM and a Hill coefficient of 4.7 for wild-type CaM. CaM1 and CaM2 shifted the Ca^{2+}-response curves to the right, with values for EC_{50} of 0.68 and 0.85 μM and Hill coefficients of 2.5 and 2.2, respectively. CaM34 was not different from wild-type CaM; EC_{50} value was 0.39 μM, and Hill coefficient was 4.2. *B,* Currents measured in response to voltage ramps in representative patches from oocytes coexpressing SK2 and the CaMs indicated at 0, 0.5, and 10 μM Ca^{2+}.

Table 1. Calmodulin E-F hands responsible for SK2 gating

Molecule	EC_{50} (μM)	*n*
Wild-type	0.38 ± 0.05	4.6 ± 1.3 (23)
CaM1	0.65 ± 0.06*	2.6 ± 0.4* (11)
CaM2	0.83 ± 0.12*	2.9 ± 0.4* (9)
CaM3	0.37 ± 0.03	4.9 ± 1.4 (13)
CaM4	0.41 ± 0.07	4.3 ± 0.9 (18)
CaM34	0.40 ± 0.04	4.4 ± 1.2 (4)
CaM234	1.04 ± 0.25*	2.8 ± 0.5* (14)
CaM134	0.87 ± 0.05*	2.5 ± 0.3* (7)

EC_{50} and Hill coefficient, *n*, determined from fits of the Hill equation to individual experiments. Data are presented as mean ± SD (number of patches). Asterisk indicates significance compared to wild-type CaM as described in Materials and Methods.

Ca^{2+} gating of SK2 channels results from Ca^{2+} binding to the first and second E-F hands in CaM and that either E-F hand 1 or 2 by itself is sufficient for channel activation.

A model for CaM-mediated gating

Ca^{2+}-dependent activation of SK channels was previously described as a time-homogenous Markov chain with four closed states and two open states (Hirschberg et al., 1998). This gating scheme was developed before elucidating the role of Ca^{2+}-CaM for SK channel gating. Assuming that SK channels are tetramers, the fluorescence measurements and functional data presented above suggest that CaM is bound to each α-subunit, and Ca^{2+} binding to either one or both E-F hands 1 or 2 on all four CaM molecules results in channel gating. This is analogous to the model developed by Zagotta et al. (1994a,b) to describe voltage-dependent gating of *Shaker* K^+ channels in which two voltage-dependent transitions must occur in each of the four subunits. A modification of this model was adopted to describe Ca^{2+}-dependent gating of SK2 (Fig. 5, *inset*). Two differences were incorporated to account for our results. First, to simulate Ca^{2+} binding to CaM, the on-rate constants were made Ca^{2+}-dependent, and all rate constants were voltage-independent. Second, the channel was allowed to enter the open state if each CaM molecule was bound with at least one Ca^{2+} molecule. To account for the cooperative interaction between the two E-F hands as suggested by the single and triple E-F hand mutations (Table 1), the off-rate for the second Ca^{2+} bound to CaM was decreased compared to the off-rate for the first bound Ca^{2+}. When each CaM molecule is bound with one or two Ca^{2+} ions, the channel can enter the open state with the rate constants determined from single-channel analysis for the open state with the longest mean open time (Hirschberg et al., 1998); functionally the five open states, O_1-O_5, are identical. The model was used to simulate Ca^{2+} gating and qualitatively accounts for the EC_{50} and Hill coefficient when both Ca^{2+}-binding domains are functional as well as when the second Ca^{2+}-dependent forward rate constant was set to zero to simulate either CaM1, CaM2, CaM234, or CaM134 (Fig. 5). The EC_{50} and Hill coefficient of 1.1 μM and 2.3, respectively, agrees well with the values determined for CaM234 (Table 1). However, the Hill coefficient determined for the complete model, 3.5, was slightly smaller than the experimentally determined value of 4.6 for wild-type CaM (Table

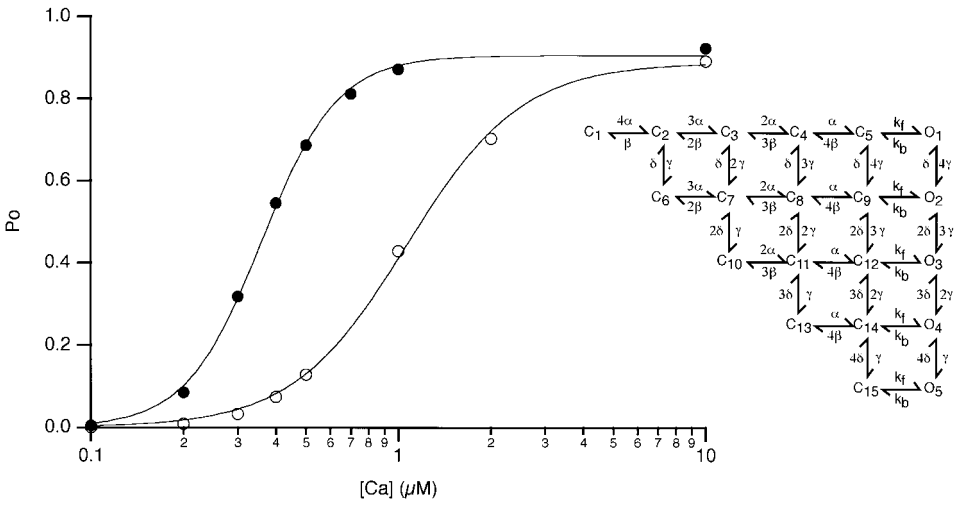

Figure 5. A model describing Ca^{2+}-dependent gating of SK2. *Inset,* The complete form of the model showing the conformational changes in the channel. C_n represents n of 15 closed states, and O_n represents n of five identical open states. The forward rate constants between the closed states, α and γ, were Ca^{2+}-dependent and given the same value of $[Ca^{2+}] \cdot 100$ μM/sec. The back rate constants, β and δ, were assigned values of 100 and 18 sec^{-1}, respectively. These values were selected based on single-channel kinetics (Hirschberg et al., 1998), EC_{50} for Ca^{2+} (Table 1), and kinetics of activation and deactivation (Xia et al., 1998). The rate constants into and out of the open state, k_f and k_b, were taken from Hirshberg et al. (1998) for the long duration open state, 1200 and 100 sec^{-1}, respectively. Plotted at Ca^{2+} concentrations similar to those used to measure Ca^{2+} gating of SK channels are simulated P_o values equal to $O_1 + O_2 + O_3 + O_4 + O_5$ for the complete model (*filled circles*), and when γ was assigned a value of zero to eliminate binding of the second Ca^{2+} to each CaM molecule, simulating CaM1 or CaM2 (*open circles*). The simulated values were fit to a Hill equation yielding an EC_{50} value of 0.36 μM and a Hill coefficient of 3.5 for the complete model and 1.1 μM and 2.3, respectively, for the abbreviated model.

1).This discrepancy may result from subtle distinctions between the EC_{50} of CaM1 and CaM2, or CaM134 and CaM234 which were not incorporated into the model.

DISCUSSION

CaM is an exquisite Ca^{2+} sensor that mediates a wide range of intracellular signaling pathways. Ca^{2+}-binding to CaM induces conformational alterations that expose domains that mediate interaction with target proteins; the activity of these substrates is altered after Ca^{2+}–CaM binding. Structurally, CaM has globular N- and C-terminal domains, each containing two E-F hand motifs separated by a flexible linker region. All four E-F hand Ca^{2+}-binding domains possess high affinity for Ca^{2+}. However, slight affinity differences and highly cooperative Ca^{2+} binding endow CaM with the ability to distinguish small fluctuations in intracellular Ca^{2+} levels within physiological ranges (Klee, 1988). After Ca^{2+} binding, the flexible tether region bends, bringing the globular domains into spatial proximity and forming a hydrophobic interface for binding to target peptides (O'Neil and DeGrado, 1990; Finn and Forsen, 1995; Finn et al., 1995). Previously, we have shown that CaM is constitutively associated with the channel α subunits and Ca^{2+} binding to CaM induces channel gating. Here, we present evidence showing structural changes in the α subunit after CaM binding and subsequent Ca^{2+} binding to the CaM–α subunit complex. We also present evidence for a modular structure to CaM; distinct regions are responsible for Ca^{2+}-dependent and Ca^{2+}-independent interactions with SK α subunits.

Structural motifs that bind Ca^{2+}-bound CaM are characterized by regularly spaced hydrophobic amino acids, and frequently have an overall positive net charge. Most of the high-affinity Ca^{2+}–CaM-binding domains conform to the 1-8-14 motif (Rhoads and Friedberg, 1997). The hydrophobic residues at these positions may interact with hydrophobic patches exposed in the N- and C-terminal domains of CaM after Ca^{2+} binding. In other instances, CaM binds to target proteins such as neurogranin (Baudier et al., 1991), neuromodulin (Alexander et al., 1988), and unconventional myosins (Wolenski, 1995) or the *Drosophila* protein *igloo* (Neel and Young, 1994), with greater affinity in absence of bound Ca^{2+}. These interactions remain Ca^{2+}-sensitive, and it is likely that the Ca^{2+}-free form of CaM performs an alternative allosteric regulatory function. A structural motif that mediates Ca^{2+}-free CaM binding, the IQ motif, is found in a variety of proteins and comprises a 14 residue stretch beginning with IQ and containing positively charged residues at positions 6 and 11. The distinction between motifs that bind Ca^{2+}-free or Ca^{2+}-bound CaM is not absolute, because some IQ motifs also conform to Ca^{2+}-dependent motifs (Rhoads and Friedberg, 1997). The interaction between SK2 α subunits and CaM is different and resembles phosphorylase kinase in which, even in the absence of Ca^{2+}, CaM is an intrinsic subunit of the enzyme, requiring harsh, denaturing conditions for subunit separation (Picton et al., 1980; Kee and Graves, 1986).

The determinants for Ca^{2+}-independent, constitutive binding to the SK2 α subunits ABC domain reside in the C-terminal half of CaM, as demonstrated by yeast two-hybrid experiments. Further analysis showed that two noncontiguous stretches of amino acids, 78–85 spanning the border of the flexible tether region with the C-terminal globular domain and the final five residues, 143–148, were both necessary for Ca^{2+}-independent binding. The Ca^{2+}-binding integrity of E-F hands 3 and 4 was not required. Two methionines within the final five residues have been implicated in Ca^{2+}–CaM binding as part of hydrophobic methionine puddles that form interfaces with target substrates (O'Neil and DeGrado, 1989, 1990). Two conserved, positively charged residues in the C domain of the channel α subunits are important for Ca^{2+}-independent CaM binding. Interestingly, charge reversal of the individual amino acids had no effect, but together, neither channel gating nor Ca^{2+}-independent CaM binding to the ABC domain was detected. The modular nature of the interactions are emphasized by this mutant because Ca^{2+}-dependent interactions are maintained even though Ca^{2+}-independent interactions have been disrupted. Apamin binding showed that the double mutant α subunits are assembled and inserted into the plasma membrane.

Ca^{2+}-dependent channel gating is mediated by Ca^{2+} binding to E-F hands 1 and 2 in the N-terminal globular domain. Mutations that reduce or eliminate Ca^{2+} binding to E-F hands 3 and 4 do not affect Ca^{2+}-gating, but the same mutations in E-F hands 1 or 2 result in shifts in apparent Ca^{2+} affinity and gating

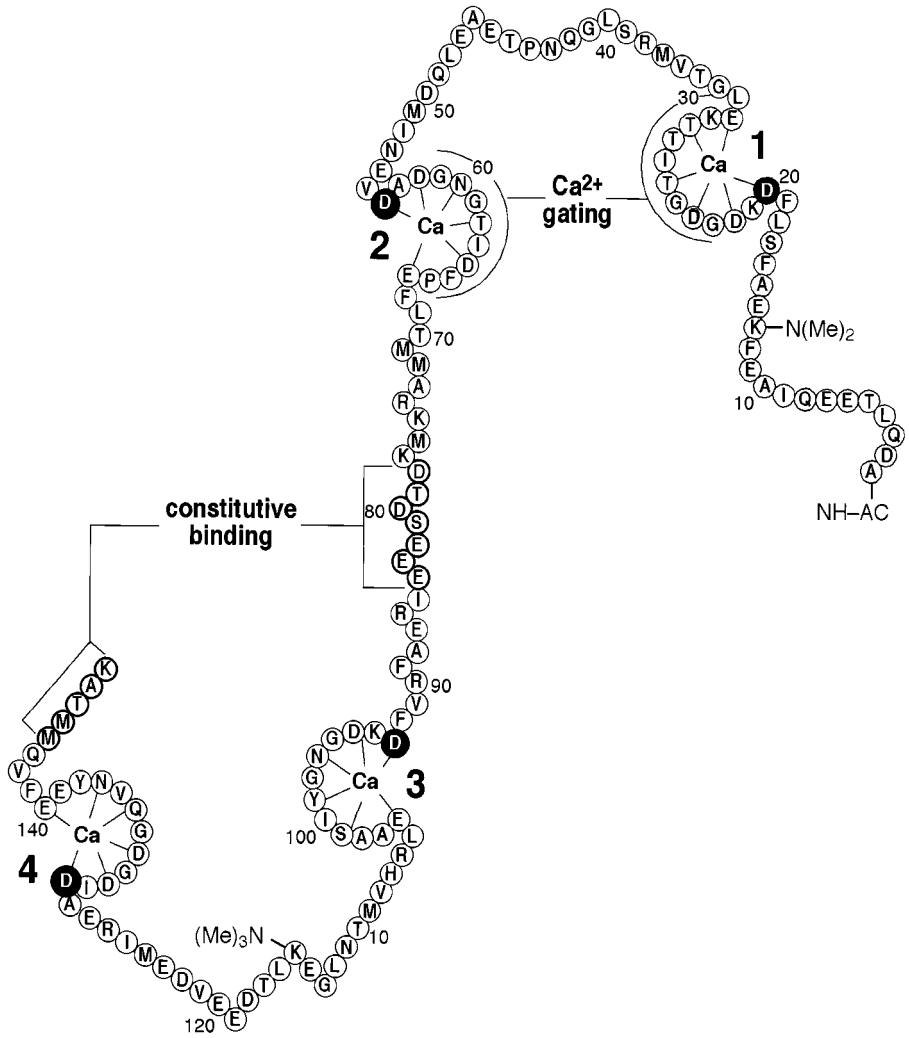

Figure 6. Schematic of CaM. E-F hands 1 and 2 are responsible for Ca^{2+}-dependent gating in SK2 channels, whereas the two indicated separate domains in the C-terminal half of CaM are necessary for Ca^{2+}-independent, constitutive binding. Aspartate residues at the first position of each E-F hand are shown as *black, filled circles*. Design based on Saimi and Kung (1994).

cooperativity. These results were unexpected because under physiological conditions, E-F hands 3 and 4 possess the highest intrinsic Ca^{2+} affinity; in most cases Ca^{2+} ions are likely bound first to these motifs and subsequently to E-F hands 1 and 2 (Wang et al., 1985). This result differs from our previous work that implicated E-F hands 3 and 4 in Ca^{2+} gating (Xia et al., 1998). The molecules employed in the present study have been repeatedly examined by nucleotide sequence analysis, and the experiments have been performed many times in different batches of oocytes. The results have been consistent and show that E-F hands 1 and 2 are necessary and sufficient for Ca^{2+} gating. Results from expression of CaMs with only E-F hands 1 or 2 intact show that a single functional E-F hand is necessary and sufficient for Ca^{2+} gating. This suggests that gating cooperativity may in part result from interactions between α subunits and not only from Ca^{2+} binding to CaM. The residues on the α subunits responsible for mediating Ca^{2+}-dependent interactions with CaM have not yet been identified despite mutagenesis of many charged and hydrophobic residues.

The picture that emerges is one in which CaM interacts in a modular way with the SK channels, the C-terminal domain mediating constitutive binding and the N-terminal domain transmitting Ca^{2+} dependence (Fig. 6).

The first evidence that CaM affects ion channels came from point mutations in *Paramecium* CaM, the *pantophobiacs*, which eliminate a calcium-activated potassium current (Schaefer et al., 1987). Interestingly, all of the *pantophobiac* mutations occur in the C-terminal globular domain of the protein, and all but two change residues in E-F hands 3 or 4 (Saimi and Kung, 1994). In our studies, the ability of these E-F hands to bind Ca^{2+} was not important for channel gating. However, the exact *pantophobiac* mutations were not examined. One *pantophobiac* mutation, M476V, resides in a small stretch implicated in Ca^{2+}-independent CaM binding. Although this is a conservative substitution, it eliminates a methionine, supporting the hypothesis that "methionine puddles" form the basis for many important hydrophobic interactions with CaM binding targets (O'Neil and DeGrado, 1990). CaM mutants in *Paramecium* also indicated distinctions among the N- and C-terminal domains for their ability to regulate ion channels; N-terminal mutants (*fast-2* or *paranoiac*) affected a Ca^{2+}-activated Na^{+} current (Kink et al., 1990). In *Drosophila*, CaM-null mutants are viable as larvae because of persistent maternal CaM. As maternal CaM levels decrease, the larvae demonstrate behavioral abnormalities strikingly similar to the avoidance behavior of *pantophobiac* mutants in *Paramecium*. Moreover, flies harboring a mutation in CaM E-F hand 1 exhibit enhanced neurotransmitter release in low Ca^{2+} (Heiman et al., 1996; Arredondo et al., 1998), consistent with a shift in the Ca^{2+} concentration–response for SK channels.

Until recently, CaM has generally been considered a mediator

of intracellular Ca^{2+} signaling pathways. However, it is now clear that CaM also plays a central role in regulating membrane potential and ion channel activity. In addition to the finding that CaM is the intrinsic Ca^{2+}-sensing subunit of SK2 channels, CaM binds to voltage-dependent L-type calcium channels through an IQ motif on the C-terminal domain of the channel, a region analogous to the region bound by CaM in SK2 channels, and plays a direct and important role in regulating L-type Ca^{2+} channel kinetics (Zühlke et al., 1999; Peterson et al., 1999). Similar to results presented for SK2 (Xia et al., 1998), the Ca^{2+}-dependent interaction of L-type Ca^{2+} channels with CaM cannot be inhibited by peptide competitors or compounds such as calmidizolium, although it is not yet clear that CaM binds constitutively to L-type Ca^{2+} channels in the quantitative absence of Ca^{2+}. Similar to the interaction of CaM with SK channels, the different E-F hand motifs make distinct contributions to L-type Ca^{2+} channel regulation (Peterson et al., 1999). In many neurons, such as hippocampal pyramidal neurons (HPNs), blockade of L-type Ca^{2+} channels also blocks the slow AHP (Tanabe et al., 1998). Moreover, in HPNs, L-type Ca^{2+} channels and SK channels reside in close proximity, and a direct functional coupling has been demonstrated (Marrion and Tavalin, 1998). By affecting L-type Ca^{2+} channel activity, SK channel activity will also be altered, exerting strong effects on spike frequency adaptation and neuronal excitability.

CaM has also been implicated in regulating the activity of ionotropic receptors such as NMDA receptors through direct interactions (Ehlers et al., 1996). Ca^{2+} flux through NMDA receptors impacts long-term potentiation, which is also coupled to CaM through activation of CaM kinase II (Otmakhov et al., 1997). Thus, CaM may be viewed as a central coordinator for a variety of ion channels, all of which influence and are influenced by Ca^{2+} dynamics and have significant long-term effects in the CNS.

REFERENCES

Alexander KA, Wakim BT, Doyle GS, Walsh KA, Storm DR (1988) Identification and characterization of the calmodulin-binding domain of neuromodulin, a neurospecific calmodulin-binding protein. J Biol Chem 263:7544–7549.

Arredondo L, Nelson HB, Beckingham K, Stern M (1998) Increased transmitter release and aberrant synapse morphology in a Drosophila *Calmodulin* mutant. Genetics 150:265–274.

Babu YS, Sack JS, Greenhough TJ, Bugg CE, Means AR, Cook WJ (1985) Three-dimensional structure of calmodulin. Nature 315:37–40.

Baudier J, Deloulme JC, Dorsselaer AV, Black D, Matthes HW (1991) Purification and characterization of a brain-specific protein kinase C substrate, neurogranin (p17). Identification of a consensus amino acid sequence between neurogranin and neuromodulin (GAP43) that corresponds to the protein kinase C phosphorylation site and the calmodulin-binding domain. J Biol Chem 266:229–237.

Blatz AL, Magleby KL (1987) Calcium-activated potassium channels. Trends Neurosci 10:463–467.

Chevray PM, Nathans D (1992) Protein interaction cloning in yeast: identification of mammalian proteins that react with the leucine zipper of Jun. Proc Natl Acad Sci USA 89:5789–5793.

Ehlers MD, Zhang S, Bernhardt JP, Huganir RL (1996) Inactivation of NMDA receptors by direct interaction of calmodulin with the NR1 subunit. Cell 84:745–755.

Fabiato A, Fabiato F (1979) Calculator programs for computing the composition of the solutions containing multiple metals and ligands for experiments in skinned muscle cells. J Physiol (Lond) 75:463–505.

Finn BE, Forsen S (1995) Minireview: the evolving model of calmodulin structure, function and activation. Structure 3:7–11.

Finn BE, Evenas J, Drakenberg T, Waltho JP, Thulin E, Forsen S (1995) Calcium-induced structural changes and domain autonomy in calmodulin. Nat Struct Biol 2:777–783.

Geiser JR, van Tuinen D, Brockerhoff SE, Neff MM, Davis TN (1991) Can calmodulin function without binding calcium? Cell 65:949–959.

Heiman RG, Atkinson RC, Andruss BF, Bolduc C, Kovalick GE, Beckingham K (1996) Spontaneous avoidance behavior in *Drosophila* null for calmodulin expression. Proc Natl Acad Sci USA 93:2420–2425.

Hille B (1992) Ionic channels of excitable membranes. Sunderland, MA: Sinauer.

Hirschberg B, Maylie J, Adelman JP, Marrion NV (1998) Gating of recombinant small conductance Ca-activated K^+ channels by calcium. J Gen Physiol 111:565–581.

Horton RM, Hunt HD, Ho SN, Pullen JK, Pease LR (1989) Engineering hybrid genes without the use of restriction enzymes: gene splicing by overlap extension. Gene 77:61–68.

Ishii TM, Maylie J, Adelman JP (1997) Determinants of apamin and D-tubocurarine block in SK potassium channels. J Biol Chem 272:23195–23200.

Kee SM, Graves DJ (1986) Isolation and properties of the active γ subunit of phosphorylase kinase. J Biol Chem 261:4732–4737.

Kink JA, Maley ME, Preston RR, Ling K-Y, Wallen-Friedman MA, Saimi Y, Kung C (1990) Mutations in paramecium calmodulin indicate functional differences between the C-terminal and N-terminal lobes *in vivo*. Cell 62:165–174.

Klee CB (1988) Interactions of calmodulin with Ca^{2+} and target proteins. In: Calmodulin (Cohen P, Klee CB, eds), pp 35–45. Amsterdam: Elsevier.

Köhler M, Hirschberg B, Bond CT, Kinzie JM, Marrion NV, Maylie J, Adelman JP (1996) Small-conductance, calcium-activated potassium channels from mammalian brain. Science 273:1709–1714.

Lakowicz JR (1983) Principles of fluorescence spectroscopy. New York: Plenum.

Lancaster B, Adams PR (1986) Calcium-dependent current generating the afterhyperpolarization of hippocampal neurons. J Neurophysiol 55:1268–1282.

Lester RAJ, Clements JD, Westbrook GL, Jahr CE (1990) Channel kinetics determine the time course of NMDA receptor-mediated synaptic currents. Nature 346:565–567.

Maconochie DJ, Zempel JM, Steinbach JH (1994) How quickly can $GABA_A$ receptors open? Neuron 12:61–71.

Madison DV, Nicoll RA (1984) Control of the repetitive discharge of rat CA1 pyramidal neurons *in vitro*. J Physiol (Lond) 354:319–331.

Marrion NV, Tavalin SJ (1998) Selective activation of Ca^{2+}-activated K^+ channels by co-localized Ca^{2+} channels in hippocampal neurons. Nature 395:900–905.

Neel VA, Young MW (1994) *Igloo*, a GAP-43-related gene expressed in the developing nervous system of *Drosophila*. Development 120:2235–2243.

O'Neil KT, DeGrado WF (1989) The interaction of calmodulin with fluorescent and photoreactive model peptides: evidence for a short interdomain separation. Proteins 6:284–293.

O'Neil KT, DeGrado WF (1990) How calmodulin binds its targets: sequence independent recognition of amphipathic α helices. Trends Biochem Sci 15:59–64.

Otmakhov N, Griffith LC, Lisman JE (1997) Postsynaptic inhibitors of calcium/calmodulin-dependent protein kinase type II block induction but not maintenance of pairing-induced long-term potentiation. J Neurosci 17:5357–5365.

Pessia M, Tucker SJ, Lee K, Bond CT, Adelman JP (1996) Subunit positional effects revealed by novel heteromeric inwardly rectifying K^+ channels. EMBO J 15:2980–2987.

Peterson BZ, DeMaria CD, Adelman JP, Yue DT (1999) Calmodulin is the Ca^{2+} sensor for Ca^{2+}-dependent inactivation of L-type calcium channels. Neuron 22:549–558.

Picton C, Klee B, Cohen P (1980) Phosphorylase kinase from rabbit skeletal muscle: identification of the calmodulin-binding subunits. Eur J Biochem 111:553–561.

Rhoads AR, Friedberg F (1997) Sequence motifs for calmodulin recognition. FASEB J 11:331–340.

Sah P (1996) Ca^{2+}-activated K^+ currents in neurons: types, physiological roles and modulation. Trends Neurosci 4:150–154.

Saimi Y, Kung C (1994) Ion channel regulation by calmodulin binding. FEBS Lett 350:155–158.

Schaefer WH, Hinrichsen RD, Burgess-Cassler A, Kung C, Blair IA, Watterson DM (1987) A mutant paramecium with a defective

calcium-dependent potassium conductance has an altered calmodulin: a nonlethal selection alteration in calmodulin regulation. Proc Natl Acad Sci USA 84:3931–3935.

Tanabe M, Gähwiler BH, Gerber U (1998) L-type calcium channels mediate the slow Ca^{2+}-dependent afterhyperpolarization current in rat CA3 pyramidal cells in vitro. J Neurophysiol 80:2268–2273.

Wang JH, Pallen CJ, Sharma RK, Adachi A-M, Adachi K (1985) The calmodulin regulatory system. Curr Top Cell Regul 27:419–436.

Weiner MP, Costa GL, Schoettlin W, Cline J, Mathur E, Bauer JC (1994) Site-directed mutagenesis of double-stranded DNA by the polymerase chain reaction. Gene 151:119–123.

Wolenski JS (1995) Regulation of calmodulin-binding myosins. Trends Cell Biol 5:310–316.

Xia X-M, Fakler B, Rivard A, Wayman G, Johnson-Pais T, Keen JE, Ishii T, Hirschberg B, Bond CT, Lutsenko S, Maylie J, Adelman JP (1998) Mechanism of calcium gating in small-conductance calcium-activated potassium channels. Nature 395:503–507.

Zagotta WN, Hoshi T, Dittman J, Aldrich RW (1994a) Shaker potassium channel gating II: transitions in the activation pathway. J Gen Physiol 103:279–313.

Zagotta WN, Hoshi T, Aldrich RW (1994b) Shaker potassium channel gating III: evaluation of kinetic models for activation. J Gen Physiol 103:321–362.

Zühlke RD, Pitt GS, Deisseroth K, Tsien RW, Reuter H (1999) Calmodulin supports both inactivation and facilitation of L-type calcium channels. Nature 399:159–162.